Experimental and Optimization Studies for the Adsorption of Cationic Dyes from Synthetic Waste Water on the Biomass of Orthophosphoric Acid Activated Barks of Prosopis Cineraria

Jayaraman, Sangeetha*+; Thiruvenkadam, Venugopal

Department of Chemistry, Government College of Engineering, Salem-600 011, INDIA

ABSTRACT: *The sorption ability of readily available barks of Prosopis cineraria (PCAC) activated by orthophosphoric acid was investigated through the effect of various process parameters such as initial dye concentration [50 to 200 mg/L], contact time, solution pH (3 to 10), and temperature [298K to 328K] and optimized using Response Surface Methodology (RSM). The physiochemical activation process was used to yield a sample with a Brunauer-Emmett-Teller (BET) surface area of 7.024 m²/g. The Activated carbon was characterized by using FT-IR and SEM. The various adsorption isotherms and kinetic models were used to interpret the experimental data. Good agreement was found between the experimental results and predicted values by RSM and about 88%, 70%, and 93% of removal efficiencies were achieved for cationic (Methylene Blue (MB), Rhodamine B (RHB), and Rhodamine 6G (RH6G) dyes with concentration 70 mg/L.*

KEYWORDS: *Sorption; Activated; Isotherm; Kinetic; Response Surface Methodology; Cationic dyes.*

INTRODUCTION

The dyes were water-soluble and intensely coloured substances and were used for the coloration of industries. The effluent of such dye industries must be treated to bring down their concentration to a permissible limit before discharging into water bodies. The colour was the most visible pollutant that can be easily recognized in wastewater and should be treated properly before discharging into water bodies or on land. The presence of colour in wastewater either in industrial or domestic needs was considered as the most undesirable one. The occurrence of various colouring agents like dyes, inorganic pigments, tannins and lignin which usually impart colour became one of the main contributors for these environmental matters with dyes wastes which were predominant. Coloured dyes are not only aesthetic, carcinogenic but also hinder light penetration [1,2] and disturb the life processes of living organisms in the water. Dyes adsorb and reflect sunlight entering the water, diminishing the photosynthesis of algae and seriously influencing the food chain. Because of their high thermal and light stability, dyes remain in the environment for a long time.

Many treatment systems have been used for the removal

** To whom correspondence should be addressed.*

+ E-mail: sangeethaj2009@gmail.com ; venupaper@gmail.com

1021-9986/2021/4/1067-1082 16/$/6.06

of synthetic dyes from aqueous solutions including ion exchange, membrane filtration, precipitation, photocatalytic degradation, oxidation, electrochemical, and adsorption. Among several dye removal techniques, adsorption is an efficient one to remove different kinds of dyes from water and wastewater [3, 4] and it has wide applicability in wastewater treatment. This process is simple to design, easy to operate, cost-effective, eco-friendly, and insensitive to toxic substances.

In the present investigation, experiments were carried out to explore a low-cost adsorbent to remove basic (cationic) dyes from the aqueous solutions. The eco-friendly nature of biomasses, their availability, and low cost were the main advantages of these resources, which made them a suitable precursor for activated carbon preparation. Activated carbons having high specific porosity, high surface areas were extremely versatile adsorbents of major industrial significance. The investigation was designed to study the adsorption of different dyes on activated carbon at various conditions in order to gain an insight into the adsorption mechanism for the cationic dyes on activated carbon.

Optimization study using Response Surface Methodology (RSM) was an experimental design that aimed to reduce the cost of expensive analysis. RSM was a collection of statistical and useful mathematical techniques for developing, improving, and optimizing the process. Recently, RSM has been applied to optimize and evaluate interactive effects of independent factors in numerous chemical and biochemical processes. RSM was also used to evaluate the relative significance of several process parameters in the presence of complex interactions. The main objective of RSM was to determine the optimum operating conditions of the process or a region that satisfies the operating specification. Besides that, RSM was considered as an efficient, cost-effective method to model and optimize bioprocess as it enabled the researchers to identify interactions between different study parameters with few possible experiments [5]. RSM was one of the most popular used methods in experimental design for the study of biosorption literature for heavy metal removal and dye removal [6-8].

In this study, the bark of Prosopis cineraria-derived activated carbon (PCAC) was used as an adsorbent for the removal of cationic dye and optimization was done by Central Composite Design (CCD) in RSM. The optimized conditions developed from the model were validated using experimental results and the feasibility of PCAC for the adsorption of dyes MB, RHB, and RH6G was obtained. Therefore, this study aimed to investigate the potential of Prosopis cineraria bark, an abundantly available solid waste, as a nonconventional adsorbent in the removal of dyes from the aqueous solutions.

EXPERIMENTAL SECTION

The barks of Prosopis cineraria were collected in the around rasipuram area in Tamil Nadu. The collected barks were washed with distilled water to remove the surface adhering particles and were sun-dried for 48 h to reduce the moisture content. They were crushed and sieved to a particle size of (1 to 2) mm. The image of Prosopis cineraria is given below.

Preparation of adsorbent

The powder of Prosopis cineraria barks was activated in two stages. The first stage involved refluxing the barks powder and 50% phosphoric acid in water (4:1 ratio of acid solution to barks powder) for 60 min, at 80 ^{o}C, following which the slurry was concentrated by evaporation. Then the slurry was cooled and used in the next stage. In the second stage, the slurry was heated in a stainless steel reactor, under flowing nitrogen at atmospheric pressure and held for 60 min at a final Heat Treatment Temperature (HTT) of 650^{o}C. The activated carbon was then cooled and stored in air tight container for further use.

Preparation of adsorbate

1g of each dye was dissolved in water and made up to 1000mL to get 1000ppm of solution which was taken as the stock solution. It was stored in a reagent bottle for making the other dilute solutions.

Characterization of adsorbent

The surface morphology of PCAC was examined with the help of Scanning Electron Microscopy (SEM). The Fourier-Transform InfraRed (FT-IR) spectroscopy of PCAC was obtained for the analysis of functional groups present on the surface of the adsorbent. The spectra were obtained in the range of 4000-400 cm^{-1} using PerkinElmer Spectrum Version 10.03.09 KBr pellets which contained PCAC. Quanta chrome Nova-1000 surface analyzer was used to determine the surface area and porosity measurements under liquid nitrogen temperature.

Effect of adsorption parameters

Effect of contact time

Contact time of PCAC with dye was one of the main factors for influenced the adsorption efficiency. Fig. 3 shows the effect of contact time on the adsorption of dyes on PCAC. It was studied in the range of 0 – 180 min for all the dyes. It could be concluded that the adsorption process reached an equilibrium state within 60 min for MB, 70 min for RH6G, and 110 min for RHB at 298K. Therefore, 60 min, 70 min, and 110 min were chosen as the optimized time for MB, RH6G, and RHB respectively.

Effect of temperature and pH

Effect of Temperature on adsorption efficiency was tested with various temperature (298K, 308K, 318K, and 328K) ranges. Fig. 4 shows that the absorption rate increases with the increasing temperature.

Another important parameter in the adsorption process was solution pH. 0.1N HCl and 0.1N NaOH were used to adjust the pH of the dye solutions. Fig. 5 shows the adsorption rate for cationic dyes on the surface of PCAC with different pH range (3, 5, 8 and10).

Adsorption experiment

In this study, the removal of dyes was tested under various conditions. The conditions like solution pH, amount of adsorbent, contact time were studied for the removal of dyes by batch method. A mechanical shaker was used and 5mL of dye sample was taken in a test tube and desired amount of adsorbent was weighed and then added to the test tube. The constant temperature was maintained throughout the experiment. Then, the adsorbents were separated from the sample by using filter paper. The absorbance was measured for a supernatant solution using UV-Vis Spectrophotometer ELICO SL159. The final concentration of dye was estimated with the help of these absorbance data. For determining the uptake of the dye, all-inclusive sets of experiments were performed at every 10 min time intervals, pH (3~10) and temperature (298K-328K). The amount of adsorption at equilibrium time, q_e (mg/g) was calculated using Eq. (1).

$$q_e = \frac{(C_o - C_e)V}{W} \quad (1)$$

Where, C_O is the liquid-phase concentrations of dye at initial condition (mg/L); C_e, is the liquid-phase concentrations of dye at equilibrium condition (mg/L); V is the volume of the solution, (L); W is the mass of the dry adsorbent used, (g).

Desorption experiment

Desorption of MB, RHB, and RH6G from PCAC was performed using ethanol. In this serial desorption experiments, MB, RHB, and RH6G containing ethanol were removed by centrifugation, and fresh ethanol was added every 2 min to prevent the re-adsorption of the above dyes on the adsorbent. Four successive adsorption and desorption cycles were performed to determine the reusability of PCAC. The percentage desorption was determined using the following Eq. (2). [9].

$$\% \text{ Desorption} = \frac{\text{initially dye sorbed} - \text{desorbed dye}}{\text{initially dye sorbed}} \times 100 \quad (2)$$

RESULTS AND DISCUSSION

Characterization of PCAC

Fourier Transform InfraRed (FT-IR) spectroscopy

The infrared spectrum of PCAC was performed before and after the adsorption process and is shown in Fig. 1. The FT-IR spectrum was obtained quantitatively to evaluate the chemical structures of PCAC. The region of the spectrum in PCAC before the adsorption, 3384 - 3394 cm^{-1} broadband indicated the hydroxyl group (OH) [10, 13, 14]. Similarly, the regions of the spectrum, 1800 - 1658 cm^{-1} indicated the presence of carbonyl group ($C=O$) [10-12, 14], 2921-2852 cm^{-1} indicated the presence of C-H group [11, 14, 15, 16], 1576 cm^{-1} indicated N-H group [15], 1360-1385. 12 cm^{-1} indicated N-O [12, 17] group and

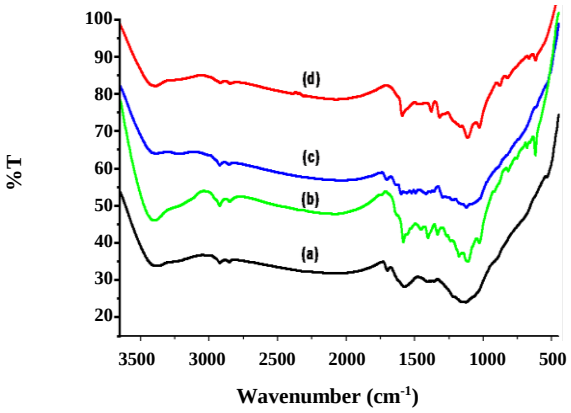

Fig. 1:FT-IR images of before (a) and after adsorption of MB (b), RHB (c), and RH6G (d) on PCAC respectively.

1126.94 cm^{-1} indicated (C-O) group [16, 18]. The various obtained new peaks and the peaks shifted in the spectrum of PCAC after adsorption of the dyes confirmed the adsorption of the dyes on the surface of PCAC. In PCAC - MB spectrum results, the regions of OH, C-H, C=O, C-O, N-O, and N=H frequencies were shifted to 3390 cm^{-1}, 2847-2073 cm^{-1}, the C=O peak disappeared due to adsorption, N-H peaks were shifted to 1590 cm^{-1}, C-O peaks were at 1114 cm^{-1} and N-O peaks were at 1380-1318 cm^{-1}. Furthermore, the newly obtained peaks at 1029 cm^{-1} (C-O), 881, 823, 666, 618 cm^{-1} (C-H) indicated the adsorption of MB on the surface of PCAC. Similarly, O-H peak in PCAC-RHB and PCAC- RH6G were shifted to 3394.56 $cm^{-1}$and 3383.35 cm^{-1}. There was no remarkable shift of C-H peaks for both RHB and RH6G dyes (2922-2847 $cm^{-1}$and 2922, 2851 cm^{-1}), the C=O peaks shifted in RH6G spectrum and were found at 1704-1600 cm^{-1}, for RHB the C=O peaks disappeared and N-H peaks were shifted to 1582 cm^{-1} for (RHB) and1560 cm^{-1} for (RH6G). The new peaks were obtained in the range of 1457 cm^{-1} and 1403 cm^{-1} corresponding to C-N group [15], 1333 cm^{-1} (N-O), 1240, 1267, 1112, 1029, 1177 cm^{-1} (C-O), 818, 681and 619 cm^{-1} (C-H bending)[17,19] for RHB and 1524 cm^{-1} (N-H), 1495, 1418, 1384 and 1362 cm^{-1} (N-O), 1295, 1222,1124 cm^{-1} (C-O) for RH6G. These remarkable changes of the IR adsorption spectrum denoted the adsorption of dyes on PCAC.

SEM

Scanning Electron Microscopy (SEM) was a tool used for characterizing the surface morphology and fundamental physical properties of the adsorbent. Fig. 2 shows the SEM of the adsorbent material which was taken before and after dye adsorption on PCAC. The SEM pictures of the adsorbed samples showed very distinguished dark spots which were taken as a sign for effective adsorption of dye molecules in the cavities and pores of this adsorbent.

BET (Brunauer-Emmett-Teller)

The textural characteristics of PCAC were presented in Table 1. Table 1 shows the minimum surface area of PCAC was 7.024 m^2/g, but the maximum bulk density of 0.932g/cc. Bulk density was an important parameter for the design of the pilot and the adsorption column. It was inversely related to the particle size of the adsorbent. The American Water Work Association has set a lower limit on the bulk density at 0.25 g/cm3 for practical use. The bulk density of PCAC was calculated as 0.932g/cc which suggested the applicability of PCAC bulk density. The bulk density was calculated as per equation 3.

$$\text{Bulk density} = \frac{\text{Mass of dry sample (g)}}{\text{Totel volume used (mL)}} \quad (3)$$

Effect of contact time

The results of the effect of contact time were revealed that the adsorption of dyes on the adsorbent was relatively faster and it was shown in Fig3. The complete adsorption equilibrium between the two phases was obtained after 60 min for MB, 70 min for RH6G (70 mg/L), and 110 min for RHB (70mg/L) at 298K. The fast adsorbate molecules uptakes by the adsorbent were due to their highly porous and mesh-like structure. The contact time determined the adsorption efficiency [20] and it can be inferred that the PCAC was very efficient since it had low contact time. There was no notable change in adsorption after equilibrium state and equilibrium concentration was attained.

Effect of temperature

The adsorption capacity of PCAC in various temperatures (at 298K, 308K, 318K, and 328K) was carried out in a constant temperature bath in solution and 0.005g of PCAC in 5mL of solution with dye concentration (50-200) mg/L.

The adsorption capacity of MB, RHB, and RH6G dyes on PCAC was observed in the following decreasing order RH6G≈MB >RHB. Fig. 4 represents the percentage of adsorption

Table 1: The textural characteristics of PCAC.

BET surface area	Pore volume	Bulk Density	Cross section
7.024 m^2/g	0.01 cc/g	0.932g/mL	16.2 A^2

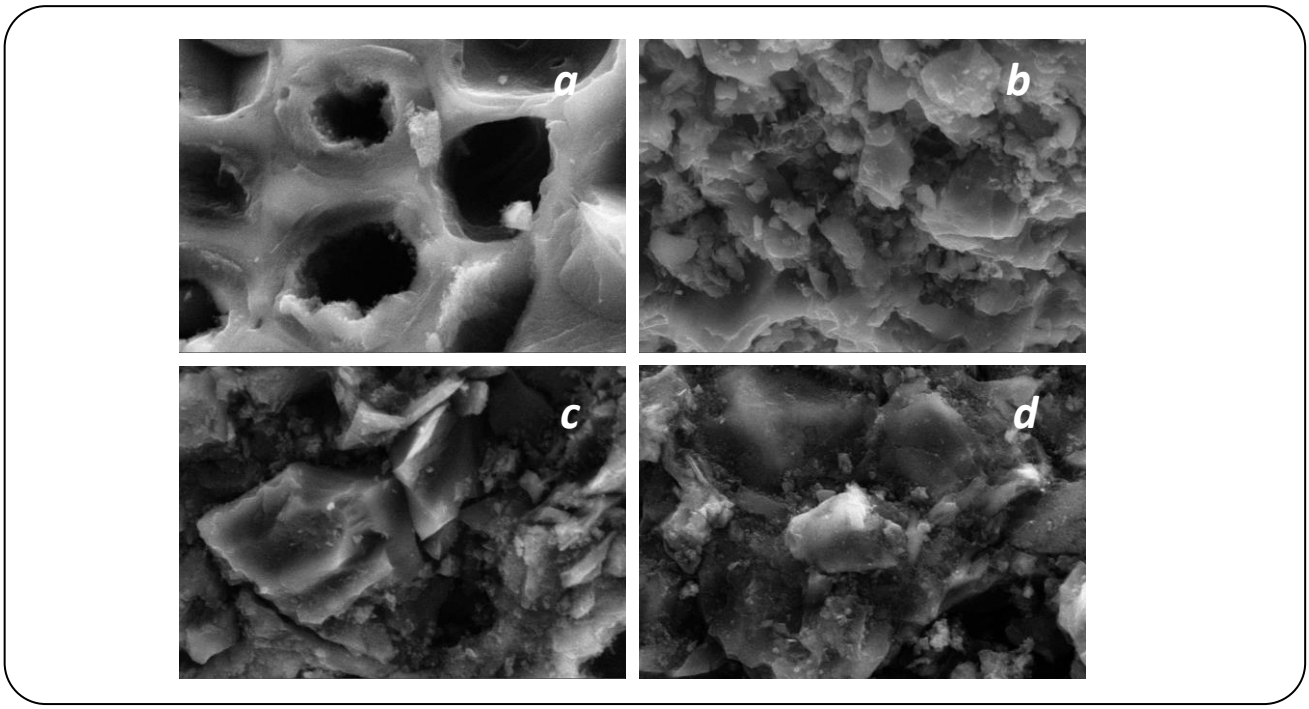

Fig. 2: SEM images of PCAC. (a) represents before and (b), (c) and (d) represents after adsorption of RH6G, RHB and MB dyes respectively.

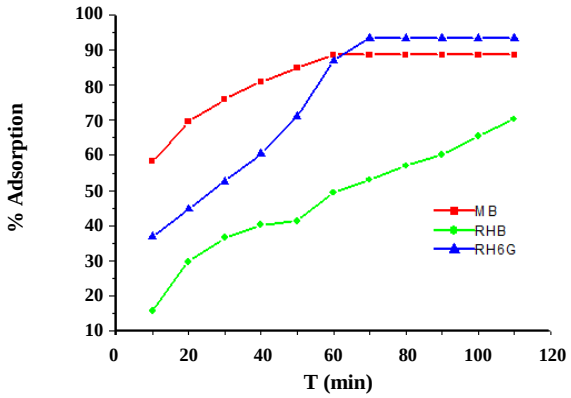

Fig 3. Effect of contact time for the adsorption of dyes with 70 mg/L concentration on PCAC at room temperature.

at various temperatures for MB, RHB, and RH6G dyes. It showed the dye saturation level of PCAC at higher temperatures was attained in short time intervals whereas a long time interval was needed for the carbon saturation of dyes at lower temperature states [21].

Effect of pH

The effect of pH on dye adsorption was checked at the solution pH 3, 5, 8, and 10 at 298K with dye concentration (50-200) mg/L.The solution pH was adjusted using 0.1N NaOH and 0.1 N HCl solutions by using a pH meter with a combined pH electrode.

This effect of pH was investigated for 3 hrs. The result showed that the maximum adsorption of RHB was obtained at the lowest solution pH 3 while the lowest adsorption was at solution pH 10. In higher solution pH, dimmer formation of RHB occurred, hence it could not enter the pores of the adsorbent due to its bigger size [22]. But the cationic dyes, such as MB, RH6G were attracted to the negatively charged surface [23] of PCAC at higher solution pH (pH 10). Therefore, the adsorption rates were improved with the changing solution of pH values from 3.0 to 10, since the number of the negatively charged sites, were increasing for MB and RH6G. Fig. 5 indicates the effect of pH on the adsorption of dyes on PCAC.

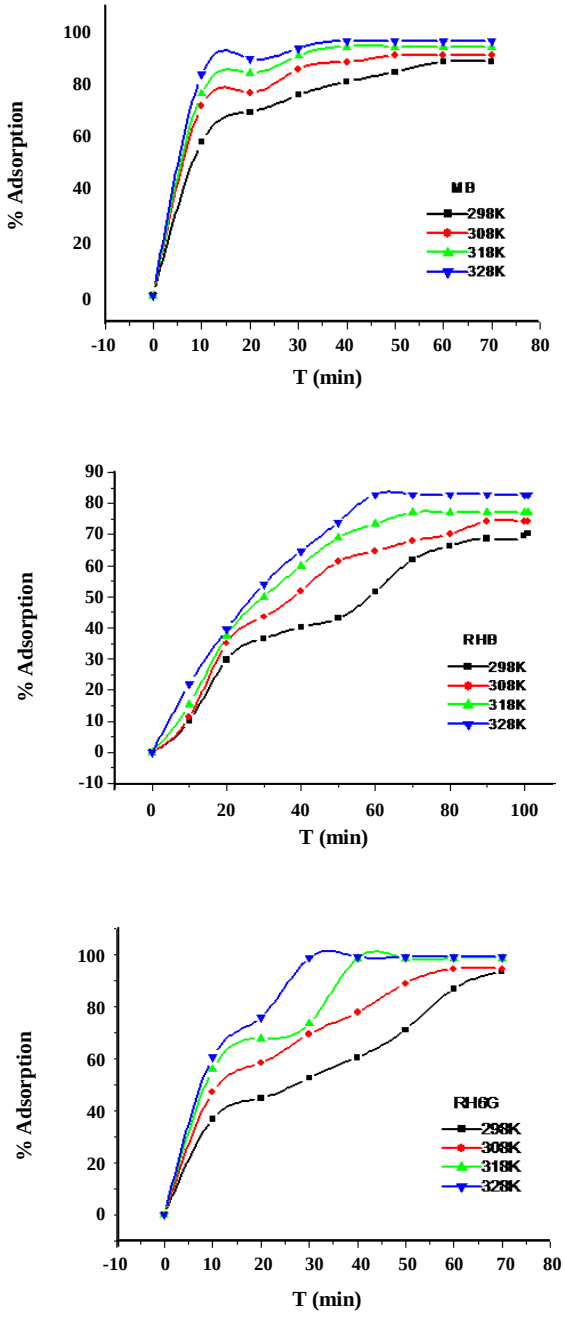

Fig 4: Percentage of adsorption of dyes with 70 mg/l concentration at various temperature ranges (298K to 328K).

Adsorption isotherms

The Langmuir isotherm was used to describe the dependence of the surface coverage of an adsorbed gas by the pressure of the gas above the surface at a fixed temperature. It provided a useful insight into the concentration dependence of the extent of surface adsorption.

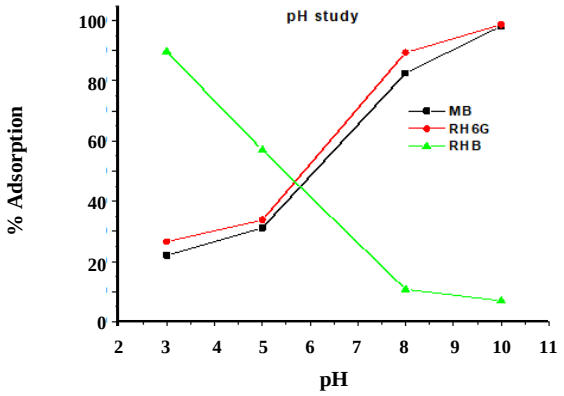

Fig 5: Percentage of adsorption of dyes with 70 mg/L concentration at different pH levels (298K).

The basic assumptions of Langmuir isotherm were the formation of a monolayer and the homogeneous sites available on the adsorbent surface [24]. Based upon these assumptions, the Langmuir represented the following linear form Eq. (4).

$$\frac{C_e}{q_e} = \frac{1}{q_m} + \frac{1}{q_m \times K_L} \quad (4)$$

where C_e and q_e are the equilibrium concentration and amount of metal adsorbed per gram of the adsorbent at equilibrium (mg/g). Q_m is the maximum monolayer coverage capacity (mg/g), K_L is the Langmuir isotherm constant (L/mg).

Furthermore, a separation factor (R_L) further explained the Langmuir isotherm:

$$R_L = \frac{1}{1 + bCo} \quad (5)$$

Where b is Langmuir constant and C_o is initial dye concentration. If $R_L>1$, the process was not favorable; when $R_L=1$, the process was linear; when $R_L=0$, the process was irreversible in nature and when $0<R_L>1$, the process was favorable. In the present investigation, the value R_L was less than one for all three dyes which showed that the adsorption process was favorable.

Fig. 6 shows a linearized plot of C_e / q_e against C_e. The values of Q_e and K_L were calculated and given in Table 2. From the values, it was concluded that the monolayer of dye molecules was formed on the adsorbent surface with constant energy and there was no transmission of dye molecules on the adsorbent surface. Further, it confirmed the endothermic nature of the processes involved in the system.

Table 2: Various parameters for isotherm models for the adsorption study of MB, RHB and RH6G dyes on the PCAC at 328K.

DYES	LANGMUIR MODEL				FREUNDLICH MODEL		
	Q_m mg/g	K_L l/g	R^2	R_L	K_F l/g	1/n	R^2
MB	250	0.166	0.952	0.1-0.029	21.12	0.41	0.990
RHB	200	0.043	0.914	0.32-0.1	8.07	0.501	0.963
RH6G	200	0.714	0.979	0.02-0.006	36.96	0.268	0.981

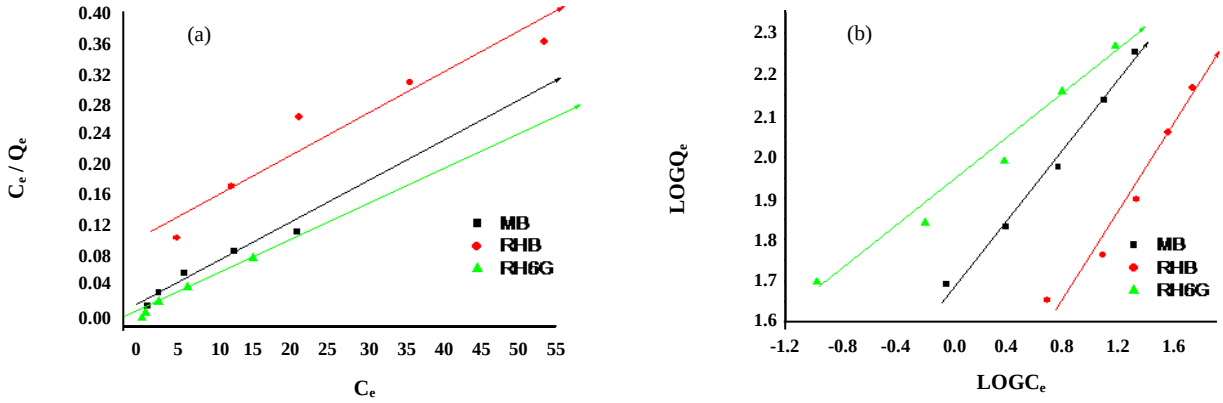

Fig 6: Adsorption isotherms. (a) and (b) are the Langmuir and Freundlich isotherm models at 328K

The Langmuir isotherm fitted with the experimental data with a good correlation coefficient of 0.952 for MB, 0.914 for RHB dye, and 0.979 for RH6G.

Freundlich assumed the heterogeneous surface energies [24]. The linearized form of freundlich isotherm was given as,

$$\log q_e = \log K_F + \frac{1}{n} \quad (6)$$

From the data in table 2, it was seen that the values of 1 / n indicated that the sorption of dyes on PCAC was favorable and the R^2 values were 0.990, 0.963, and 0.981 for MB, RHB, and RH6G respectively. Furthermore, if the value of 'n' was above unity, the adsorption was a favorable physical process. Here the 'n' values were found to be 2.42, 1.99, and 3.73 for MB, RHB, and RH6G dyes respectively and they showed favorable physical adsorption.

It was quite clear from the R^2 values that fit adsorption isotherm were found to be the Freundlich isotherm for all three dyes.

It could be concluded that the Freundlich isotherm model showed a better mathematical fit with the experimental data than the Langmuir model (based on the higher correlation coefficient (R^2) for all dyes. The isotherms data were shown in Table 2 and Fig. 6 (a,b).

Adsorption kinetics

The kinetics of adsorption of various dyes on the PCAC was evaluated using standard kinetic models like pseudo-first-order and pseudo-second-order. Furthermore, the Weber-Morris model fitted with the data to analyze the diffusion of dye on the adsorbent which was shown in Fig. 7 (c, d, and e).

The kinetics studies were useful not only for the determination of the equilibrium time of an adsorption process but also for designing the treatment systems based on the reaction rate. The rate of adsorption for all three dyes was high at the initial times of adsorption. For those dyes, most of the adsorption took place within 10 min which indicated that the rate of dye adsorption by PCAC was high. The rate of adsorption became slower with time and reached a constant value (equilibrium time). The initial faster rate was due to the availability of the uncovered surface area of the adsorbents. The result of fitting was listed in Table 3.

Table 3: Kinetic parameters for the adsorption of dyes on the adsorbent (PCAC).

Dyes	model Pseudo first order			Pseudo second order model			Weber-Morris model	
	K_1 g/mg.min	Qe mgg^{-1}	R^2	K_2 g/mg.min	H mgg^{1}.min	R^2	K_{id} mgg^{-1} $min^{1/2}$	R^2
MB	0.077	19.93	0.988	0.0059	30.30	0.999	2.795	0.994
RHB	0.047	75.51	0.977	0.00008	1.76	0.998	9.31	0.999
RH6G	0.242	575.28	0.826	0.000735	7.35	0.975	9.35	0.932

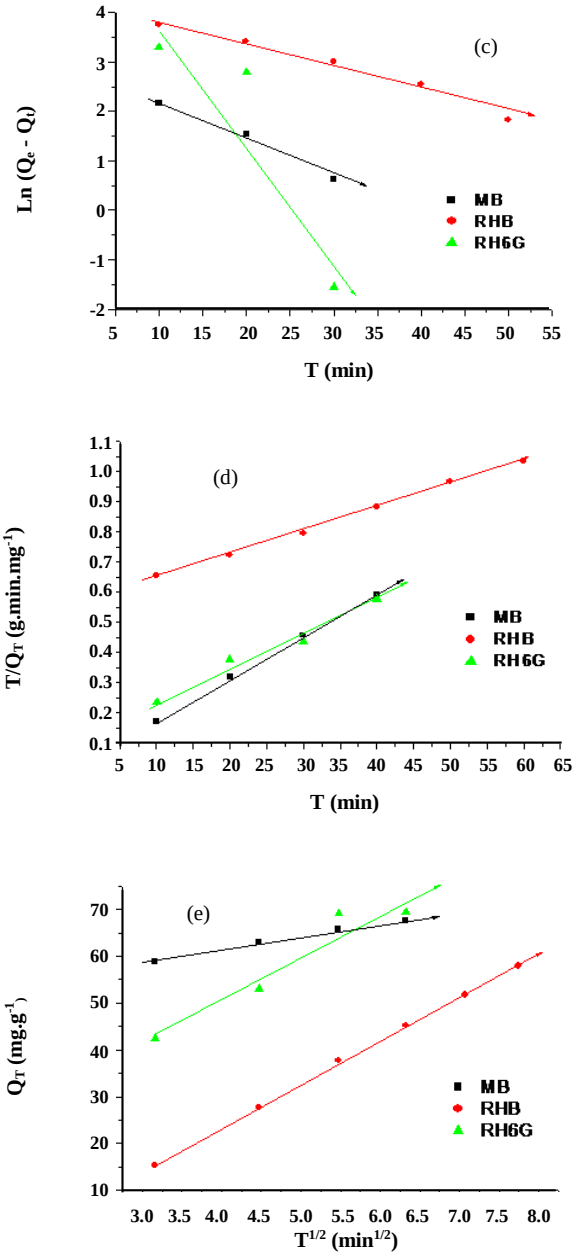

Fig 7: Kinetic models (c), (d), and (e) are the pseudo-first, pseudo-second-order, and Weber-Morris models.

The equation for the models used for the kinetic studies were given below,

$$\text{Pseudo-first order} - \log(q_e - q_t) = \log q_t - \frac{k_1}{2.303}t \quad (7)$$

$$\text{Pseudo-second order} = \frac{t}{q_t} = \frac{1}{K_2 q_e} + \frac{1}{q_e}t \quad (8)$$

$$\text{Weber-Morris model} - q_t = K_{id}t^{0.5} \quad (9)$$

Where k_1 (min^{-1}) is pseudo-first-order adsorption rate constant, q_t (mg/g) is the amount of sorption at time *t* (min), q_{eq} (mg/g) is the amount of sorption at equilibrium, k_1 and q_{eq} values were obtained from the plots of $\log(q_e - q_t)$ versus t, K_2 (g/mg min) is adsorption rate constant, K_2 and q_e were obtained from the intercept and slope of the plot of t/qt versus t [9]. K_{dif} is rate constant of intraparticle diffusion (mg g-1 $min^{-0.5}$), C is the intercept of intraparticle diffusion and R^2 is Correlation coefficient [25].

Weber-Morris model: The mechanism of the adsorption could be determined by the Weber-Morris model[25]. It explained the migration of the dye molecules from the aqueous solution to the adsorbent surface *via* the intraparticle diffusion method.

The plot of q_t versus $t_{1/2}$ yielded a linear relationship in which the values of K_{dif} and C were calculated from the slopes and intercept; the corresponding values were presented in Table 10. The R^2 (0.994, 0.999, and 0.932) values (Table 3) closer to unity suggested the applicability of this kinetic model and that the intraparticle diffusion process was the rate-limiting step for MB, RHB, and RH6G.

The best kinetic model was selected based on the highest correlation coefficient (R^2) and that it was related to the pseudo-second-order adsorption model. Additionally, the value of q_e (cal) was calculated by pseudo-second-order model which was very close to that of the experimental value, q_e (exp) in Table 3. Accordingly,

Table 4: Thermodynamic parameters of PCAC.

DYES	ΔH^0 KJ/mol	ΔS^0 KJ/mol	ΔG^0 KJ/mol			
			298K	308K	318K	328K
MB	81.62	0.31	- 5.082	-5.932	-7.476	-9.110
RHB	21.34	0.18	-2.139	-2.713	-3.198	-4.283
RH6G	143.43	0.53	-6.573	-7.255	-11.116	-12.983

the pseudo-second-order model was predominant for describing the dye adsorption mechanism on the PCAC.

All the experimental data showed better compliance with the pseudo-second-order kinetic model for PCAC. The higher correlation coefficient values (R^2) of the three dyes were 0.999, 0.998, and 0.975. Moreover, the values of Q_e for the dyes were 71, 142.86, and 100 (MB, RHB, and RH6G) respectively.

Thermodynamic parameters

The thermodynamic parameters of adsorption were shown in Table 4. They were calculated from the following equations:

$$K_D = \frac{C_s}{C_e} \quad (10)$$

$$\Delta G^\circ = -RT\ln K_D \quad (11)$$

$$\ln K_D = \frac{\Delta S^\circ}{R} - \frac{\Delta H^\circ}{RT} \quad (12)$$

where K_D is the equilibrium constant (l/g), C_S is the amount of dye adsorbent (mg/g) [26], C_e is the equilibrium concentration of dye in the solution (mg/L), R is the gas constant (8.314 mol/K and T is the absolute solution temperature (K). The plot of lnKc vs. 1/T was linear (Fig. 8).

The effect of temperatures (25ºC, 35ºC, 45ºC, 55ºC) for different dye solutions on the adsorption kinetics was studied to determine the optimum solution temperature and the thermodynamic behavior of MB, RHB, and RH6G dyes on PCAC. The amount of dye adsorption increased with the increasing temperature of the solution which in turn indicated an endothermic nature. The more negative values of ΔG^0 indicated that the adsorption process was spontaneous. The thermodynamic parameters were calculated as per the equations [27-28]. The positive values of ΔH^0 and ΔS^0 also indicated

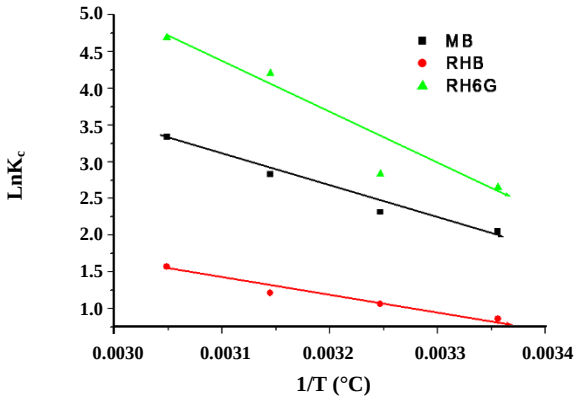

Fig 8: Plot of LnK_C Vs 1/T.

the endothermic nature and randomness at the solid-solution interface which occurred in the internal structure of the adsorbent. The ΔH^0 values less than 25 indicated that the physical adsorption was the most important process in the mechanism of adsorption [21]. The ΔH^0 and ΔS^0 values for dyes were 81.62 and 0.31 for MB, 21.34 and 0.18 for RHB, and 143.43 and 0.53 for RH6G respectively as shown in Table 4.

Optimized Adsorption condition

Response Surface Methodology (RSM)

The Response Surface Methodology (RSM) used several independent variables and their interaction with the dependent variables to form a mathematical and statistical equation. The optimization of the dye removal by the activated carbon was studied using Response Surface Methodology (RSM) [29]. The Central Composite Design (CCD) was selected for this work since it was the most used second-order statistical method which gave a complete optimization with less number of experimental runs[29,30]. Three types of points were used in CCD: 1. Cube point, 2. Center point and 3. Axial point. The number of factorial runs required was 2^n, 2n experimental runs for axial point, where n is the number of variables

Table 5: Independent experimental variables used in CCD.

Variable	Units	-α (-2)	Low(-1)	Central(0)	High (+1)	+α (+2)
Concentration of dye	Mg/L	36.7	100	200	300	363.3
Time	min	50.5	60	75	90	99.5
Temperature	K	304.8	308	313	318	321.2

used in the experiment. Equation 13 gives the number of experiments that are required for the analysis by the CCD

Number of experiments = $2^n + 2n + C$

$$\text{Number of experiments} = 2^n + 2n + C \quad (13)$$

Where *C* is the number of runs for Central point.

In this work, CCD was used to optimize the removal percentage of all three dyes by the activated carbon. The number of variables was fixed at 3. The independent experimental variables used in the CCD were the concentration of the dye, time of contact between the dye and the activated carbon, and the experimental temperature. The pH of the solution was not used to design CCD since it was found that at a particular pH only the removal efficiency was maximum and also that Rhodamine B shows maximum removal at acidic pH when compared to the other dyes which showed the maximum removal at basic pH.

Equation (13) gives the number of experiments for obtaining the valid results from CCD. 2^3 experiments were run for the factorial points, 6 runs were carried out to determine the axial points and 6 replicates were carried out for the central point data. Totally 20 experiments were carried out with each dye. Since all three dyes showed the approximately similar result of the removal percentage, only 1 design was used for all the dyes. The average results of the triplicate were used as a response in this study. The independent experimental variables and their coded values are given in Table 5.

The percentage removal of the dye was the response for CCD and the experimental results are presented in Table 6. The quadratic equation and ANNOVA table were used to study the interaction, usefulness, and accuracy of CCD model were used for best fit, Minitab 17 was also used [30].

The equation that was used to predict the removal of the dyes obtained from the central composite design was given in Equations (14) to (16).

$$\%\ \text{removal of MB} = -3131 - 1.362\,\text{Concentration} - 6.80\,\text{Time} + 22.67\,\text{Temperature} + 0.000224\,\text{Concentration} \times \text{Concentration} - 0.008058\,\text{Time} \times \text{Time} - 0.04027\,\text{Temperature} \times \text{Temperature} - 0.000267\,\text{Concentration} \times \text{Time} + 0.003980\,\text{Concentration} \times \text{Temperature} + 0.02710\,\text{Time} \times \text{Temperature} \quad (14)$$

$$\%\ \text{removal of RB} = -2702 - 1.277\,\text{Concentration} - 5.58\,\text{Time} + 19.57\,\text{Temperature} + 0.000234\,\text{Concentration} \times \text{Concentration} - 0.00895\,\text{Time} \times \text{Time} - 0.03481\,\text{Temperature} \times \text{Temperature} - 0.000512\,\text{Concentration} \times \text{Time} + 0.003745\,\text{Concentration} \times \text{Temperature} + 0.02373\,\text{Time} \times \text{Temperature} \quad (15)$$

$$\%\ \text{removal of RB6} = -2383 - 1.126\,\text{Concentration} - 5.078\,\text{Time} + 17.28\,\text{Temperature} + 0.000211\,\text{Concentration} \times \text{Concentration} - 0.007772\,\text{Time} \times \text{Time} - 0.03065\,\text{Temperature} \times \text{Temperature} - 0.000331\,\text{Concentration} \times \text{Time} + 0.003253\,\text{Concentration} \times \text{Temperature} + 0.02148\,\text{Time} \times \text{Temperature} \quad (16)$$

The accuracy of the model, the importance of each variable, and their interaction were determined by the Analysis of variance (ANNOVA) [30]. F-test with a confidence limit 95% ($P<0.05$) was taken to test the model for its significance and lack of fit. Generally, the higher the F value and lower the p-value indicated the best fit of the model towards the removal of dye from the wastewater. The error analysis of the model was determined using mean square and the sum of square values. The model had a low mean

Table 6: Experimental design matric for the removal of dyes by the activated carbon.

S. No	Concentration (mg/L)	Time (min)	Temperature (K)	% of removal of MB	% of removal of RHB	% of removal of RH6G
1	300	90	308	79.58	78.45	79.26
2	200	75	313	84.08	82.65	84.13
3	200	75	313	84.25	82.45098	84.1
4	300	60	318	75.45	74.65	75.42
5	100	60	308	84.47	83.42	83.75
6	100	90	318	96.51	95.62	97.12
7	200	75	313	82.71	81.25	82.9
8	300	60	308	70.65	69.52	70.69
9	100	90	308	91.54	90.86	92.45
10	100	60	318	77.85	76.5	80.12
11	300	90	318	89.05	86.14	88.58
12	200	75	313	82.65	81.95	82.68
13	200	75	321.165	83.75	83.75	85.15
14	36.7	75	313	98.55	97.87	97.89
15	200	75	313	84.98	83.5	85.1
16	200	75	313	84.78	84	85.49
17	200	75	304.835	79.45	77.65	79.85
18	200	50.505	313	68.45	67.25	69.01
19	200	99.495	313	90.45	88.05	90.75
20	363.3	75	313	81.95	80.65	82.45

square values and the sum of square values of errors showed statistically significant results. The results of ANNOVA are presented in Tables 7 to 9.

R^2 values for the modeling of the removal of dye from the wastewater using CCD have given information for the prediction of the results using the regression equation. Table 10 provides the information of R^2 of the model. It was found that, for all the dyes, CCD modeling showed a value of nearly 99.5% (0.995) indicating that the predicted values and the experimental values were close to each other and only 0.5% of the total variation was not explained. It was interesting to note that the prepared activated carbon showed the same efficiency for all three dyes. The lack of fit for the P values was 0.003, 0.061, and 0.016 for Methylene blue, Rhodamine B, and Rhodamine 6G respectively which suggested that the application of this model for the removal of the dyes has been significantly high.

The ANNOVA results are given in table 7 to 9 and it could be inferred from the table that all the dyes fitted into the CCD model. The F values for all the dyes were high and from the F test, it could be inferred that the order of fitness was Rhodamine 6G >Methylene blue > Rhodamine B. From the P-value which was approximately zero for all the dyes indicated that all the dyes fitted well with the CCD mode [31]. Concentration, temperature, and time showed a high significant value for the removal of dyes as indicated by the low P-value and large F values. Among

Table 7: Results of the analysis of variance of Central Composite Design model for the adsorption of Methylene blue dye from wastewater into the activated carbon.

Source	Degree of freedom	Adjusted Sums of Squares	Adjusted Mean Squares	F-Value	P-Value
Model	11	1065.14	96.830	198.28	0.000
Blocks	2	11.32	5.660	11.59	0.004
Linear	3	855.78	285.258	584.12	0.000
Concentration	1	295.30	295.295	604.67	0.000
Time	1	531.54	531.544	1088.43	0.000
Temperature	1	28.94	28.935	59.25	0.000
Square	3	132.03	44.010	90.12	0.000
Concentration*Concentration	1	66.09	66.088	135.33	0.000
Time*Time	1	43.41	43.408	88.88	0.000
Temperature*Temperature	1	13.38	13.385	27.41	0.001
2-Way Interaction	3	66.01	22.003	45.06	0.000
Concentration*Time	1	1.28	1.280	2.62	0.144
Concentration*Temperature	1	31.68	31.681	64.87	0.000
Time*Temperature	1	33.05	33.048	67.67	0.000
Error	8	3.91	0.488		
Lack-of-Fit	5	3.87	0.774	64.07	0.003
Pure Error	3	0.04	0.012		
Total	19	1069.04			

Table 8: Results of analysis of variance of Central Composite Design model for the adsorption of Rhodamine B dye from wastewater into the activated carbon.

Source	Degree of freedom	Adjusted Sums of Squares	Adjusted Mean Squares	F-Value	P-value
Model	11	1065.69	96.881	142.08	0.000
Blocks	2	13.88	6.940	10.18	0.006
Linear	3	847.64	282.548	414.37	0.000
Concentration	1	324.33	324.330	475.65	0.000
Time	1	491.42	491.422	720.70	0.000
Temperature	1	31.89	31.893	46.77	0.000
Square	3	146.06	48.685	71.40	0.000
Concentration*Concentration	1	72.29	72.291	106.02	106.02
Time*Time	1	53.57	53.572	78.57	78.57
Temperature*Temperature	1	10.00	10.004	14.67	14.67
2-Way Interaction	3	58.11	19.370	28.41	0.000
Concentration*Time	1	4.71	4.712	6.91	0.030
Concentration*Temperature	1	28.05	28.050	41.14	0.000
Time*Temperature	1	25.35	25.347	37.17	0.000
Error	8	5.45	0.682		
Lack-of-Fit	5	5.07	1.013	7.80	0.061
Pure Error	3	0.39	0.130		
Total	19	1071.15			

Table 9: Results of analysis of variance of Central Composite Design model for adsorption of Rhodamine 6G dye from waste water into the activated carbon.

Source	Degree of freedom	Adjusted Sums of Squares	Adjusted Mean Squares	F-Value	P-Value
Model	11	1039.45	94.496	216.78	0.000
Blocks	2	8.44	4.221	9.68	0.007
Linear	3	872.10	290.699	666.89	0.000
Concentration	1	313.99	313.990	720.32	0.000
Time	1	515.82	515.820	1183.33	0.000
Temperature	1	42.29	42.286	97.01	0.000
Square	3	115.02	38.339	87.95	0.000
Concentration*Concentration	1	58.80	58.801	134.89	0.000
Time*Time	1	40.38	40.382	92.64	0.000
Temperature*Temperature	1	7.75	7.752	17.78	0.003
2-Way Interaction	3	43.90	14.632	33.57	0.000
Concentration*Time	1	1.97	1.970	4.52	0.066
Concentration*Temperature	1	21.16	21.158	48.54	0.000
Time*Temperature	1	20.77	20.769	47.65	0.000
Error	8	3.49	0.436		
Lack-of-Fit	5	3.39	0.677	20.18	0.016
Pure Error	3	0.10	0.034		
Total	19	1042.94			

Table 10: Model summary of the Central Composite Design model for adsorption of dye from wastewater into the activated carbon.

Dye	S	R^2	R^2 adjusted	R^2 for prediction
MB	0.698	99.63%	99.13%	95.24%
RHB	0.825752	99.49%	98.79%	94.48%
RH6G	0.660230	99.67%	99.21%	96.28%

the three variables studied, time seemed to show the highest significance which in turn could be inferred from the large F values. The order of significance of the individual variables was time > concentration> temperature. The dual interaction effects were studied and it was found that all the variables had a high dual interaction effect as shown by the P values which was less than 0.05. Two-way interaction between the variables was also studied and it was found that except for the concentration-time interaction which showed p values greater than 0.05 for Rhodamine 6G and methylene blue, all other interactions showed p values less than 0.05. So it was concluded that the model was favorable for predicting the removal of all the three dyes by the activated carbon within the choice of the variable values studied.

The CCD was used to optimize the condition for the removal of dye by keeping the target removal as 99%. The results of the model are given in Table 11. The experiments were carried out to validate the condition and the results were presented in table 10. The experiment results validated that the model has given in an error of less than 3% for all the dye for optimization. From Table 11 it can be inferred that the temperature of about 320K was the optimum condition for the removal of all the dyes and

Table 11: Conditions for optimization of removal of dyes from the wastewater by CCD model (for 99% removal).

Dye	Concentration (mg/L)	Time (Min)	Temperature (K)	Experimental Results for the removal of dye
Methylene blue	98	100	320	97.25
Rhodamine B	110	100	320	96.98
Rhodamine 6G	48	90	320	97.32

time was nearly 100 minutes for methylene blue and Rhodamine B removal. However, the time of 90 minutes and concentration of 40 ppm were optimum for the Rhodamine 6G removal. The highest concentration of removal was seen in Rhodamine B with 110mg/L.

CONCLUSIONS

In this study, phosphoric acid activated biomass of Prosopis cinereia barks was used as a low-cost adsorbent for the removal of cationic dyes like methylene blue, rhodamine 6g, and rhodamine b from aqueous solution with higher adsorption capacity. The adsorption of all the dyes followed Freundlich isotherm and Pseudo-second order kinetics. The thermodynamic study demonstrated the spontaneous and endothermic nature of the adsorption process due to the negative values of ΔG^0 and positive values of ΔH^0. Based on the result of adsorption, CCD explained the adsorption efficiency of PCAC.

Received : Nov. 13, 2019 ; Accepted : May 4, 2020

REFERENCES

[1] Mahmoodabadi, M., Khoshdast, H., Shojaei, V., Efficient Dye Removal from Aqueous Solutions Using Rhamnolipid Biosurfactants by Foam Flotation, *Iranian Journal of Chemistry and Chemical Engineering (IJCCE)*, **38 (4)**: 127-140 (2019)

[2] Shabaan, O. A., Jahin, H. S., Mohamed, G. G., Removal of Anionic And Cationic Dyes from Wastewater By Adsorption Using Multiwall Carbon Nanotubes, *Arabian Journal of Chemistry*, **13(3)**: 4797-4810 (2020)

[3] Kamranifar, M., Naghizadeh, A., Montmorillonite Nanoparticles In Removal of Textile Dyes from Aqueous Solutions: Study of Kinetics and Thermodynamics, *Iranian Journal of Chemistry and Chemical Engineering (IJCCE)*, **36(6)**: 127-137 (2017).

[4] Sharma Y.C., Upadhyay S.N., An Economically Viable Removal of Methylene Blue by Adsorption on Activated Carbon Prepared from Rice Husk, *The Canadian Journal of Chemical Engineering*, **89(2)**: 377-383 (2011).

[5] Jain M., Garg V.K., Kadirvelu K., Investigation of Cr (VI) Adsorption onto Chemically Treated Helianthus Annuus: Optimization Using Response Surface Methodology, *Bioresource Technology*, **102(2)**: 600-605 (2011).

[6] Ghorbani F., Kamari S., Application of Response Surface Methodology for Optimization of Methyl Orange Adsorption by Fe-Grafting Sugar Beet Bagasse, *Adsorption Science & Technology*, **35(3-4):** 317-338 (2017).

[7] Ngoh Y.Y., Leong Y.H., Gan C.Y., Optimization Study for Synthetic Dye Removal Using an Agricultural Waste of Parkia Speciosa Pod: a Sustainable Approach for Waste Water Treatment, *International Food Research Journal*, **22(6)**: 2351-2357 (2015).

[8] Sadhukhan B., Mondal N.K., Chattoraj S., Optimisation Using Central Composite Design (CCD) and the Desirability Function for Sorption of Methylene Blue from Aqueous Solution onto Lemna Major, *Karbala International Journal of Modern Science*, **2(3)**: 145-155 (2016).

[9] Yousaf M., Ahmad M., Ahmad B.I., Nasir A., Removal of RY42 Anionic Dye Pollutant from Aqueous Solution Using Novel Reusable Adsorbent Prepared from water Chestnut Peel and Fruit, *International Journal of Current Engineering and Technology. :* - (2018).

[10] Jawad A.H., Razuan R., Appaturi J.N., Wilson L.D., Adsorption and Mechanism Study for Methylene Blue Dye Removal with Carbonized Watermelon (Citrullus Lanatus) Rind Prepared Via One-Step Liquid Phase H2SO4 Activation, *Surfaces and Interfaces*, **16**: 76-84 (2019).

[11] Jawad A.L.I., Al-Heetim D.T., Abd Rashid R., Biochar from Orange (Citrus Sinensis) Peels by Acid Activation for Methylene Blue Adsorption, *Iranian Journal of Chemistry and Chemical Engineering*, **38(2)**: 91-105 (2019)

[12] Jawad A.H., Ismail K., Ishak M.A.M., Wilson L.D., Conversion of Malaysian Low-Rank Coal to Mesoporous Activated Carbon: Structure Characterization and Adsorption Properties, *Chinese Journal of Chemical Engineering*, **27(7)**: 1716-1727 (2019).

[13] Saka C., Şahin Ö., Celik M.S., The Removal of Methylene Blue from Aqueous Solutions by Using Microwave Heating and Pre-Boiling Treated Onion Skins as a New Adsorbent. Energy Sources, Part A: Recovery, *Utilization, and Environmental Effects*, **34(17)**: 1577-1590 (2012).

[14] Laskar, N. and Kumar, U., SEM, FTIR and EDAX Studies for the Removal of Safranin Dye from Water Bodies using Modified Biomaterial-Bambusa Tulda. In IOP Conference Series, *Materials Science and Engineering*, **225(1)**: 012105, IOP Publishing (2017).

[15] Du Y., Pei M., He Y., Yu F., Guo W., Wang L., Preparation, Characterization and Application of Magnetic Fe_3O_4-CS for the Adsorption of Orange I from Aqueous Solutions, *PloS one*, **9(10)**: 108647 (2014).

[16] Nasr J.B., Hamdi N., Elhalouani F., Characterization of Activated Carbon Prepared from Sludge Paper for Methylene Blue Adsorption, *Journal of Materials and Environmental Sciences*, 1960-1967 (2017).

[17] Shamsuddin, M.S., Yusoff, N.R.N., Sulaiman, M.A., Synthesis and Characterization of Activated Carbon Produced from Kenaf core Fiber Using H_3PO_4 Activation. *Procedia Chemistry*, **19**: 558-565 (2016).

[18] Das, D., Samal, D.P., Meikap, B.C., Preparation of Activated Carbon from Green Coconut Shell and Its Characterization, *Journal of Chemical Engineering & Process Technology*, **6(5)**: 1-7 (2015)

[19] Al-Qodah, Z., Shawabkah, R., Production and Characterization of Granular Activated Carbon from Activated Sludge. *Brazilian Journal of Chemical Engineering*, **26(1)**: 127-136 (2009).

[20] Pathania, D., Sharma, S., Singh, P., Removal of Methylene blue by Adsorption onto Activated Carbon Developed from Ficus Carica Bast, *Arabian Journal of Chemistry*, **10**: S1445-S1451. (2017).

[21] Gupta, V.K., Pathania, D., Sharma, S., Adsorptive Remediation of Cu (II) and Ni (II) by Microwave Assisted H_3PO_4 Activated Carbon. *Arabian Journal of Chemistry*, **10**: S2836-S2844 (2017).

[22] Jinisha, R., Gandhimathi, R., Ramesh, S.T., Nidheesh, P.V., Velmathi, S., Removal of Rhodamine B Dye from Aqueous Solution by Electro-Fenton Process Using Iron-Doped Mesoporous Silica as a Heterogeneous Catalyst. *Chemosphere*, **200**: 446-454 (2018).

[23] Arastehnodeh, A., Saghi, M., Khazaei Nejad, M., Preparation, Characterization and Application of Nanospherical α-Fe_2O_3 Supported on Silica for Photocatalytic Degradation of Methylene Blue. *Iran. J. Chem. Chem. Eng. (IJCCE)*, **38(2)**: 21-28 (2019).

[24] Dada, A.O., Olalekan, A.P., Olatunya, A.M., Dada, O.J.I.J.C., Langmuir, Freundlich, Temkin and Dubinin–Radushkevich Isotherms Studies of Equilibrium Sorption of Zn^{2+} unto Phosphoric Acid Modified Rice Rusk. *IOSR Journal of Applied Chemistry*, 3(1): 38-45 (2012).

[25] Ayazi, Z., Monsef Khoshhesab, Z., Amani-Ghadim, A., Synthesis of Nickel Ferrite Nanoparticles as an Efficient Magnetic Sorbent for Removal of an Azo-dye: Response Surface Methodology and Neural Network Modeling. *Nanochemistry Research*, **3(1)**: 109-123 (2018).

[26] Postai, D.L., Demarchi, C.A., Zanatta, F., Melo, D. C.C., Rodrigues, C.A. Adsorption of Rhodamine B and Methylene Blue Dyes Using Waste of Seeds of Aleurites Moluccana, a Low Cost Adsorbent, *Alexandria Engineering Journal*, **55(2)**: 1713-1723 (2016).

[27] Singha, B., Bar, N., Das, S.K., The Use of Artificial Neural Network (ANN) for Modeling of Pb(II) Adsorption in Batch Process, *Journal of Molecular Liquids*, **211**: 228-232 (2015).

[28] Neelavannan, M.G., Revathi, M., Basha, C.A., Photocatalytic and Electrochemical Combined Treatment of Textile Wash Water. Journal of Hazardous Materials, **149(2)**: 371-378 (2007).

[29] Kusuma, H.S., Sudrajat, R.G.M., Susanto, D.F., Gala, S., Mahfud, M., December. Response Surface Methodology (RSM) Modeling of Microwave-Assisted Extraction of Natural Dye from Swietenia Mahagony: A Comparison between Box-Behnken and Central Composite Design Method. *AIP Conference Proceedings*, **1699(1):** 050009 (2015).

[30] Podstawczyk, D., Witek-Krowiak, A., Dawiec, A., Bhatnagar, A., Biosorption of Copper(II) Ions by Flax Meal: Empirical Modeling and Process Optimization by Response Surface Methodology (RSM) and Artificial Neural Network (ANN) Simulation. *Ecological Engineering*, **83**:364-379 (2015).

[31] Abdulhameed, A. S., Jawad, A. H., Mohammad, A. T., Synthesis of Chitosan-Ethylene Glycol Diglycidyl Ether/TiO_2 Nanoparticles for Adsorption of Reactive Orange 16 Dye Using a Response Surface Methodology Approach. *Bioresource Technology*, **293**: 122071 (2019).